PRAMANA
— journal of
physics

Vol. 41, No. 4,
October 1993
pp. 311–327

Mathematical analysis of isobaric decay chain in alpha particle induced reactions

S MUKHERJEE, N L SINGH* and J RAMA RAO**
School of Studies in Physics, Vikram University, Ujjain 456010, India
*Physics Department, MS University, Baroda 390001, India
**Physics Department, Banaras Hindu University, Varanasi 221005, India

MS received 15 February 1993; revised 20 July 1993

Abstract. A detailed mathematical formalism is developed from the first principles, to separate out the fractional contributions of the cross-section σ_g and σ_p for the production of the two isobaric precursor nuclei- grand parent and parent, respectively, to the cross-section σ_d for the formulation of the residual nucleus of interest. The analytical work of separating out such contributions gives a meaningful picture to the comparison with the theoretical predictions of hybrid model, using the initial exciton number $n_0 = 4(4p\,0h)$.

Keywords. Isobaric precursors; decay chain; Batemann's equations; hybrid model.

PACS No. 24·90

1. Introduction

During the last decade, a great deal of experimental studies and phenomenological modelling effort has been expended in order to explain the pre-equilibrium complex particle emission in the intermediate energy nuclear reactions [1, 2]. A large number of experimental measurements of the excitation functions has been made for a better understanding of the reactions involving complex particles [3, 4]. A detailed analysis of the experimental data [5] indicates that, even if the available measurements were accurate enough, the results disagree with the theory by several orders of magnitude. One of the reasons for this discrepancy is because the excitation functions represent the combined effects of two or more different reactions which produce beta decaying isobars, leading to the actually observed residual nucleus.

The above situation is often encountered in the activation method for the determination of excitation functions for (α, pxn) and $(\alpha, \alpha xn)$ type of reactions. For example, one can see that for a given target, the $[\alpha,(x+4)n]$, $[\alpha, p(x+3)n]$ and $[\alpha, \alpha xn]$ reactions lead to residual nuclei which are isobars of one another and form a beta-decaying chain. Thus, the growth and decay of the last residual nucleus are influenced by the contributions coming from its isobaric precursors. In such cases, the simple expression [6]

$$\sigma = \frac{\lambda A_i A_\gamma}{\phi P_i W_i P_\gamma \theta_\gamma \mathrm{Nav}(1-\exp(-\lambda t_i))\exp(-\lambda tw)(1-\exp(-\lambda \Delta))}$$

cannot be used to determine the cross-section of the residual (daughter) nucleus, since it does not take into account the contributions from the decaying parent and

grandparent isobars (these include the contributions during their growth throughout the period of irradiation and also later due to their decay).

In the earlier reports on such inclusive excitation functions, no mention has been made about the possible isobaric precursor contributions [3] and no attempt has been made to account for them quantitatively. In the present work, a detailed formalism is developed from the first principles to separate out exactly, point-by-point, the isobaric precursor contributions from the measured excitation functions relevant to the particular reaction under study. This will enable a direct comparison of the theory and experiment for a single specified reaction.

With this end in view, the activation cross-section of four $(\alpha, xnypz\alpha)$ types of reactions on the target element niobium, in the energy range from threshold to 120 MeV, were adopted from our earlier measurements [5], for the analysis of isobaric precursor contributions, and to compare the results with the relevant theoretical calculations, on the basis of hybrid model [7].

2. Mathematical formalism

Let T be a target containing N_T nuclei per unit area and ϕ be the flux of α-particles incident on it for a period of time x. During this period of irradiation, three isobaric nuclei, G, P and D are produced through (α, xn), $(\alpha, px'n)$ and $(\alpha, \alpha x''n)$ reactions with cross-sections σ_g, σ_p and σ_d respectively. Also the isobaric nuclei are all radioactive with disintegration constants λ_g, λ_p and λ_d respectively and forming a radioactive decay chain

$$G \xrightarrow{\lambda_g} P \xrightarrow{\lambda_p} D \xrightarrow{\lambda_d}$$

to be designated by the notation that G stands for grandparent, P stands for parent and D for the daughter nucleus.

After a period of irradiation, x, the products are allowed to decay for a waiting time t_a and then the activity of the daughter nucleus D is measured up to the time t_b starting from t_a.

Treating T as a long-lived ($\lambda_T \simeq 0$) leading member of a (fictitious) radioactive series

$$T \underset{\sigma_g}{\xrightarrow{\lambda_T}} G \xrightarrow{\lambda_g} P \xrightarrow{\lambda_p} D \xrightarrow{\lambda_d}$$

the reaction yield of the grandparent G through (α, xn) reaction with cross-section σ_g can be simulated by using standard Batemann's equations [8] and making the substitutions,

$$T\lambda_T = \phi N_T \sigma_g$$

and

$$\lambda_T \simeq 0.$$

Similarly, the reaction yield of the parent P through $(\alpha, px'n)$ reaction with cross-section σ_p can be simulated by the (fictitious) radioactive series

$$T \underset{\sigma_p}{\xrightarrow{\lambda_T}} P \xrightarrow{\lambda_p} D \xrightarrow{\lambda_g}$$

with the following substitutions in Batemann's equations:

$$T\lambda_T = \phi N_T \sigma_p$$

and

$$\lambda_T \simeq 0.$$

Likewise the direct production of the daughter nucleus D through the reaction $(\alpha, \alpha x'' n)$ with a cross-section σ_d can be simulated by the (imaginary) radioactive series

$$T \underset{\sigma_d}{\overset{\lambda_T}{\rightarrow}} D \overset{\lambda_d}{\rightarrow}$$

with the following substitutions in Batemann's equations

$$T\lambda_T = \phi N_T \sigma_d$$

and

$$\lambda_T \simeq 0.$$

For simplicity of notation, let the letters T, G, P and D also stand for the numbers of radioactive nuclei of that kind, present at the instant of time under consideration.

The above described scenario can be schematically represented as follows:

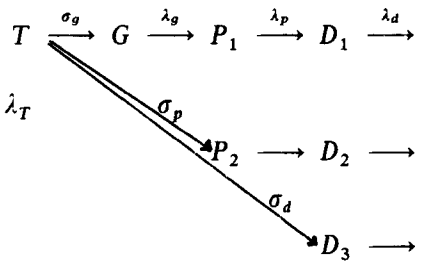

Stage 1: *Up to the end of irradiation* (x)

According to Batemann's equation,

$$G\lambda_g = (T\lambda_T)\frac{\lambda_g}{\lambda_g - \lambda_T}[1 - \exp(-(\lambda_g - \lambda_T)x)]$$

Substituting

$$\lambda_T = 0,$$

$$T\lambda_T = \phi N_T \sigma_g$$

One has

$$G_x = \frac{\phi N_T \sigma_g}{\lambda_g}(1 - \exp(-\lambda_g x)) \tag{1}$$

$$P_1\lambda_p = T\lambda_T\left[\frac{\lambda_g}{\lambda_g - \lambda_T}\frac{\lambda_p}{\lambda_p - \lambda_T}\frac{\lambda_g}{\lambda_T - \lambda_g}\frac{\lambda_p}{\lambda_p - \lambda_g}\exp(-(\lambda_g - \lambda_T)x) + \frac{\lambda_g}{\lambda_g - \lambda_p}\frac{\lambda_p}{\lambda_T - \lambda_p}\exp(-(\lambda_p - \lambda_T)x)\right].$$

Substituting

$$\lambda_T = 0,$$

$$T\lambda_T = \phi N_T \sigma_g$$

One has,

$$P_1 = \frac{\phi N_T \sigma_g}{\lambda_p}\left[1 - \frac{\lambda_p}{\lambda_p - \lambda_g}\exp(-\lambda_g x) - \frac{\lambda_g}{\lambda_g - \lambda_p}\exp(-\lambda_p x)\right] \tag{2a}$$

$$P_2\lambda_p = (T\lambda_T)\frac{\lambda_p}{\lambda_p - \lambda_T}[1 - \exp(-(\lambda_p - \lambda_T)x)]$$

Substituting

$$\lambda_T = 0,$$

$$T\lambda_T = \phi N_T \sigma_p$$

One has

$$P_2 = \frac{\phi N_T \sigma_p}{\lambda_p}(1 - \exp(-\lambda_p x)). \tag{2b}$$

Combining (2a) and (2b), one defines

$$P_x = P_1 + P_2$$

$$P_x = \frac{\phi N_T \sigma_g}{\lambda_p}\left(1 - \frac{\lambda_p}{\lambda_p - \lambda_g}\exp(-\lambda_g x) - \frac{\lambda_g}{\lambda_g - \lambda_p}\exp(-\lambda_p x)\right) + \frac{\phi N_T \sigma_p}{\lambda_p}(1 - \exp(-\lambda_p x)) \tag{3}$$

Similarly using Batemann's equations and making suitable substitutions, one gets

$$D_1 = \frac{N_T \phi \sigma_g}{\lambda_d}\left(1 - \frac{\lambda_p}{\lambda_p - \lambda_g}\frac{\lambda_d}{\lambda_d - \lambda_g}\exp(-\lambda_g x) - \frac{\lambda_g}{\lambda_g - \lambda_p}\frac{\lambda_d}{\lambda_d - \lambda_p}\exp(-\lambda_p x) - \frac{\lambda_g}{\lambda_g - \lambda_d}\frac{\lambda_p}{\lambda_p - \lambda_d}\exp(-\lambda_d x)\right) \tag{4a}$$

$$D_2 = \frac{N_T \phi \sigma_p}{\lambda_d}\left(1 - \frac{\lambda_d}{\lambda_d - \lambda_p}\exp(-\lambda_p x) - \frac{\lambda_p}{\lambda_p - \lambda_d}\exp(-\lambda_d x)\right) \tag{4b}$$

$$D_3 = \frac{N_T \phi \sigma_d}{\lambda_d}(1 - \exp(-\lambda_d x)) \tag{4c}$$

By adding (4a), (4b) and (4c), one defines

$$D_x = D_1 + D_2 + D_3$$

$$D_x = \frac{\phi N_T \sigma_g}{\sigma_d}\left(1 - \frac{\lambda_p}{\lambda_p - \lambda_g}\frac{\lambda_d}{\lambda_d - \lambda_g}\exp(-\lambda_g x) - \frac{\lambda_g}{\lambda_d - \lambda_p}\frac{\lambda_d}{\lambda_d - \lambda_p}\exp(-\lambda_p x) - \frac{\lambda_g}{\lambda_g - \lambda_d}\frac{\lambda_p}{\lambda_p - \lambda_d}\exp(-\lambda_d x)\right)$$

$$+\frac{\phi N_T \sigma_p}{\lambda_d}\left(1-\frac{\lambda_d}{\lambda_d-\lambda_p}\exp(-\lambda_p x)-\frac{\lambda_p}{\lambda_p-\lambda_d}\exp(-\lambda_d x)\right)$$

$$+\frac{\phi N_T \sigma_d}{\lambda_d}(1-\exp(-\lambda_d x)) \tag{5}$$

Stage 2: Irradiation ended, reaction is stopped. T is no longer present

$$G \xrightarrow{\lambda_g} P \xrightarrow{\lambda_p} D \xrightarrow{\lambda_d}$$

At the start of the series decay, ($t = 0$), $G = G_x$, $P = P_x$ and $D = D_x$.

$G = G_x \exp(-\lambda_g t)$ is the grandparent

To obtain P the rate equation is,

$$\frac{dP}{dt} = G\lambda_g - P\lambda_p$$

$$\exp(\lambda_p t)\left(\frac{dP}{dt}+P\lambda_p\right) = (G\lambda_g)\exp(\lambda_p t)$$

$$\frac{d}{dt}(P\exp(\lambda_p t)) = G\lambda_g \exp(\lambda_p t)$$

Integrating above equation, one gets

$$P\exp(\lambda_p t) = G_x\lambda_g \int \exp(-\lambda_g t)\exp(\lambda_p t)dt + K_p$$

$$= \frac{G_x\lambda_g}{\lambda_p-\lambda_g}\exp((\lambda_p-\lambda_g)t) + K_p$$

At $t = 0$, $P = P_x$

$$P_x = \frac{G_x\lambda_g}{\lambda_p-\lambda_g} + K_p$$

$$K_p = P_x - \frac{G_x\lambda_g}{\lambda_p-\lambda_g}$$

$$P = \frac{G_x\lambda_g}{\lambda_p-\lambda_g}(\exp(-\lambda_g t)-\exp(-\lambda_p t)) + P_x\exp(-\lambda_p t) \tag{6}$$

To solve for D, the rate equation is

$$\frac{dD}{dt} = \lambda_p P - \lambda_d D$$

$$\frac{dD}{dt} + \lambda_d D = \lambda_p P$$

$$D\exp(\lambda_d t) = \int \lambda_p P \exp(\lambda_d t)\mathrm{d}t$$

$$= \lambda_p \int \left\{ \frac{G_x \lambda_g}{\lambda_p - \lambda_g} [\exp((\lambda_d - \lambda_g)t) - \exp((\lambda_d - \lambda_p)t)] + P_x \exp((\lambda_d - \lambda_p)t) \right\} \mathrm{d}t$$

$$= \lambda_p \left[\frac{G_x \lambda_g}{\lambda_p - \lambda_g} \left\{ \frac{\exp(\lambda_d - \lambda_g)t}{(\lambda_d - \lambda_g)} - \frac{\exp(\lambda_d - \lambda_p)t)}{(\lambda_d - \lambda_p)} \right\} + \frac{P_x}{\lambda_d - \lambda_p} \exp((\lambda_d - \lambda_p)t) \right] + K_d$$

At $t = 0$, $D = D_x$

Therefore

$$K_d = D_x - \lambda_p \left[\frac{G_x \lambda_g}{\lambda_p - \lambda_g} \left\{ \frac{1}{\lambda_d - \lambda_g} - \frac{1}{\lambda_d - \lambda_p} \right\} + \frac{P_x}{\lambda_d - \lambda_p} \right]$$

Therefore

$$D = \lambda_p \left[\frac{G_x \lambda_g}{\lambda_p - \lambda_g} \left\{ \frac{\exp(-\lambda_g t)}{\lambda_d - \lambda_g} - \frac{\exp(-\lambda_p t)}{\lambda_d - \lambda_p} \right\} + \frac{P_x}{\lambda_d - \lambda_p} \exp(-\lambda_p t) \right] + D_x \exp(-\lambda_d t)$$

$$- \lambda_p \left[\frac{G_x \lambda_g}{\lambda_p - \lambda_g} \left\{ \frac{1}{\lambda_d - \lambda_g} - \frac{1}{\lambda_d - \lambda_p} \right\} + \frac{P_x}{\lambda_d - \lambda_p} \right] \exp(-\lambda_d t)$$

$$D = \lambda_p \left[\frac{G_x \lambda_g}{\lambda_p - \lambda_g} \left\{ \left(\frac{\exp(-\lambda_g t) - \exp(-\lambda_d t)}{\lambda_d - \lambda_g} \right) - \left(\frac{\exp(-\lambda_p t) - \exp(-\lambda_d t)}{\lambda_d - \lambda_p} \right) \right\} + \frac{P_x}{\lambda_d - \lambda_p} (\exp(-\lambda_p t) - \exp(-\lambda_d t)) \right] + D_x \exp(-\lambda_d t) \quad (7)$$

The number of radioactive daughter nuclei that have decayed in the time between t_a and t_b be designated as $[D_d]_{t_a}^{t_b}$. Then

$$[D_d]_{t_a}^{t_b} =$$

$$= \int_{t_a}^{t_b} \lambda_d D \mathrm{d}t = \left\{ \left[\frac{\lambda_d \lambda_p \lambda_g G_x}{\lambda_p - \lambda_g} \frac{1}{\lambda_d - \lambda_g} \left(\frac{\exp(-\lambda_g t)}{\lambda_g} - \frac{\exp(-\lambda_d t)}{\lambda_d} \right) - \frac{1}{\lambda_d - \lambda_p} \left(\frac{\exp(-\lambda_p t)}{\lambda_p} - \frac{\exp(-\lambda_d t)}{\lambda_d} \right) \right] + \frac{\lambda_p \lambda_d P_x}{\lambda_d - \lambda_p} \left(\frac{\exp(-\lambda_p t)}{\lambda_p} - \frac{\exp(-\lambda_d t)}{\lambda_d} \right) + \lambda_d D_x \left(\frac{\exp(-\lambda_d t)}{\lambda_d} \right) \right\}_{t_a}^{t_b}.$$

Therefore

$$[D_d]_{t_a}^{t_b} = G_x\lambda_g\left[\frac{\lambda_p\lambda_d(\exp(-\lambda_g t_a)-\exp(-\lambda_g t_b))}{(\lambda_p-\lambda_g)(\lambda_d-\lambda_g)}\right.$$
$$+\frac{\lambda_p\lambda_d(\exp(-\lambda_p t_a)-\exp(-\lambda_p t_b))}{(\lambda_g-\lambda_p)(\lambda_d-\lambda_p)}$$
$$\left.+\frac{\lambda_p\lambda_d(\exp(-\lambda_d t_a)-\exp(-\lambda_d t_b))}{(\lambda_g-\lambda_d)(\lambda_p-\lambda_d)}\right]$$
$$P_x\lambda_p\left[\frac{\lambda_d}{\lambda_d-\lambda_p}\left\{\left(\frac{\exp(-\lambda_p t_a)-\exp(-\lambda_p t_b)}{\lambda_p}\right)\right.\right.$$
$$\left.\left.-\left(\frac{\exp(-\lambda_d t_a)-\exp(-\lambda_d t_b)}{\lambda_d}\right)\right\}\right]$$
$$+D_x\lambda_d\left(\frac{\exp(-\lambda_d t_a)-\exp(-\lambda_d t_b)}{\lambda_d}\right)$$

$$[D_d]_{t_a}^{t_b} = \phi N_T\sigma_g(1-\exp(-\lambda_g x))\left[\frac{\lambda_p\lambda_d(\exp(-\lambda_g t_a)-\exp(-\lambda_g t_b)}{(\lambda_p-\lambda_g)(\lambda_d-\lambda_g)}\right.$$
$$+\frac{\lambda_p\lambda_d(\exp(-\lambda_p t_a)-\exp(-\lambda_p t_b))}{(\lambda_g-\lambda_p)(\lambda_d-\lambda_p)}$$
$$\left.+\frac{\lambda_p\lambda_d(\exp(-\lambda_d t_a)-\exp(-\lambda_d t_b))}{(\lambda_g-\lambda_d)(\lambda_p-\lambda_d)}\right]$$
$$+\phi N_T\sigma_g\left(1-\frac{\lambda_p}{\lambda_p-\lambda_g}\exp(-\lambda_g x)-\frac{\lambda_g}{\lambda_g-\lambda_p}\exp(-\lambda_p x)\right)$$
$$\times\left[\frac{\lambda_d}{\lambda_d-\lambda_p}\left\{\left(\frac{\exp(-\lambda_p t_a)-\exp(-\lambda_p t_b)}{\lambda_p}\right)\right.\right.$$
$$\left.\left.-\left(\frac{\exp(-\lambda_d t_a)-\exp(-\lambda_d t_b)}{\lambda_d}\right)\right\}\right]$$
$$+\phi N_T\sigma_p(1-\exp(-\lambda_p x))\left[\frac{\lambda_d}{\lambda_d-\lambda_p}\left\{\left(\frac{\exp(-\lambda_p t_a)-\exp(-\lambda_p t_b)}{\lambda_p}\right)\right.\right.$$
$$\left.\left.-\left(\frac{\exp(-\lambda_d t_a)-\exp(\lambda_d t_b)}{\lambda_d}\right)\right\}\right]$$
$$+\phi N_T\sigma_g\left[1-\frac{\lambda_p}{\lambda_p-\lambda_g}\frac{\lambda_d}{\lambda_d-\lambda_g}\exp(-\lambda_g x)-\frac{\lambda_g}{\lambda_d-\lambda_p}\frac{\lambda_d}{\lambda_d-\lambda_p}\exp(-\lambda_p x)\right.$$
$$\left.-\frac{\lambda_g}{\lambda_g-\lambda_d}\frac{\lambda_p}{\lambda_p-\lambda_d}\exp(-\lambda_d x)\right]\left(\frac{\exp(-\lambda_d t_a)-\exp(-\lambda_d t_b)}{\lambda_d}\right)$$
$$+\phi N_T\sigma_p\left[1-\frac{\lambda_d}{\lambda_d-\lambda_p}\exp(-\lambda_p x)-\frac{\lambda_p}{\lambda_\beta-\lambda_d}\exp(-\lambda_d x)\right]$$

$$\times\left(\frac{\exp(-\lambda_d t_a)-\exp(-\lambda_d t_b)}{\lambda_d}\right)$$

$$+\phi N_T\sigma_d(1-\exp(-\lambda_d x))\left(\frac{\exp(-\lambda_d t_a)-\exp(-\lambda_d t_b)}{\lambda_d}\right) \tag{8}$$

These $[D_d]_{t_a}^{t_b}$ nuclei that have decayed in the time interval between t_a and t_b, have emitted characteristic γ-rays of energy E_γ with an abundance of θ_γ per decay and these γ-rays are detected by a detector, with a photopeak efficiency P_γ corresponding to the energy E_γ and the given geometry and recorded as a full energy peak of area A_γ.

Therefore

$$A_\gamma = [D_d]_{t_a}^{t_b}\theta_\gamma P_\gamma$$

where

$$[D_d]_{t_a}^{t_b} = \frac{A_\gamma}{\theta_\gamma P_\gamma} \tag{9}$$

Also, N_T the number of target atoms per unit area is

$$N_T = \frac{w_i p_i N_{\mathrm{AV}}}{A_i} \tag{10}$$

where w_i is the weight of the target foil per unit area, P_i is the abundance of the target isotope, A_i is the mass number of the target and N_{AV} is the Avagadro number. Using (8), (9) and (10) and rearranging, one finally gets

$$\frac{A_i A_\gamma}{\phi w_i \theta_\gamma p_i P_\gamma N_{\mathrm{AV}}} = K$$

$$= \sigma_g(1-\exp(-\lambda_g x))\left[\frac{\lambda_p\lambda_d(\exp(-\lambda_g t_a)-\exp(-\lambda_g t_b))}{(\lambda_p-\lambda_g)(\lambda_d-\lambda_g)}\right.$$

$$+\frac{\lambda_p\lambda_d(\exp(-\lambda_p t_a)-\exp(-\lambda_p t_b))}{(\lambda_g-\lambda_p)(\lambda_d-\lambda_p)}$$

$$\left.+\frac{\lambda_p\lambda_d(\exp(-\lambda_d t_a)-\exp(-\lambda_d t_b))}{(\lambda_g-\lambda_d)(\lambda_p-\lambda_d)}\right] \Rightarrow g_1$$

$$+\sigma_g\left(1-\frac{\lambda_p}{\lambda_p-\lambda_g}\exp(-\lambda_g x)-\frac{\lambda_g}{\lambda_g-\lambda_p}\exp(-\lambda_p x)\right)$$

$$\times\left[\frac{\lambda_d}{\lambda_d-\lambda_p}\left(\frac{\exp(-\lambda_p t_a)-\exp(-\lambda_p t_b)}{\lambda_p}-\frac{\exp(-\lambda_d t_a)-\exp(-\lambda_d t_b)}{\lambda_d}\right)\right]$$

$$\Rightarrow g_{12}$$

$$+\sigma_g\left[1-\frac{\lambda_p}{\lambda_p-\lambda_g}\frac{\lambda_d}{\lambda_d-\lambda_g}\exp(-\lambda_g x)-\frac{\lambda_g}{\lambda_g-\lambda_p}\frac{\lambda_d}{\lambda_d-\lambda_p}\exp(-\lambda_p x)\right.$$

$$\left.-\frac{\lambda_g}{\lambda_g-\lambda_d}\frac{\lambda_p}{\lambda_p-\lambda_d}\exp(-\lambda_d x)\right]\left(\frac{\exp(-\lambda_d t_a)-\exp(-\lambda_d t_b)}{\lambda_d}\right) \Rightarrow g_{13}$$

$$+\sigma_p(1-\exp(-\lambda_p x))\left[\frac{\lambda_d}{\lambda_d-\lambda_p}\left(\frac{\exp(-\lambda_p t_a)-\exp(-\lambda_p t_b)}{\lambda_p}\right.\right.$$

$$\left.\left.-\frac{\exp(-\lambda_d t_a)-\exp(-\lambda_d t_b)}{\lambda_d}\right)\right]\Rightarrow g_2$$

$$+\sigma_p\left[1-\frac{\lambda_d}{\lambda_d-\lambda_p}\exp(-\lambda_p x)-\frac{\lambda_p}{\lambda_p-\lambda_d}\exp(-\lambda_d x)\right]$$

$$\times\left(\frac{\exp(-\lambda_d t_a)-\exp(-\lambda_d t_b)}{\lambda_d}\right)\Rightarrow g_{23}$$

$$+\sigma_d(1-\exp(-\lambda_d x))\left(\frac{\exp(-\lambda_d t_a)-\exp(-\lambda_d t_b)}{\lambda_d}\right)\Rightarrow g_3 \tag{11}$$

Therefore,

$$K=\sigma_g(g_1+g_{12}+g_{13})+\sigma_p(g_2+g_{23})+\sigma_d g_3 \tag{12}$$

Dividing throughout by g_3, one gets the experimentally measured cross-section σ_{exp} as

$$\sigma_{exp}=\frac{K}{g_3}=\sigma_g\frac{(g_1+g_{12}+g_{13})}{g_3}$$

$$+\sigma_p\frac{(g_2+g_{23})}{g_3}$$

$$+\sigma_d$$

$$\sigma_{exp}=\sigma_g C_g+\sigma_p C_p+\sigma_d$$

where C_g and C_p defined as above represent the relative cross-sectional contributions of the isobaric precursors to the daughter nucleus under study. In other words they represent the *legacy* of the grandparent and parent to the daughter isobar.

The physical significance of the terms g_1, g_{12}, g_{13}, g_2, g_{23}, and g_3 is understood by realizing that the activity of the daughter nucleus D at the final instant of time t_a just before activity measurement is contributed in six ways: Three isobars G, P and D contributing during two specific periods; (a) growth phase, from beginning to the end of irradiation ($t'=0-x$) and (b) decay phase, from the end of irradiation to the instant of counting ($t'=x-t_a$). These contributing factors are clearly explained in table 1.

3. Results and discussion

As mentioned above, the study of excitation functions is generally complicated by the possibility of isobaric precursors contributing to the cross-section of the formation of the residual nucleus of interest, particularly in the high energy region. This provides the motivation of separating out such contributions from four typical $(\alpha, xnypz\alpha)$ reactions, namely ^{93}Nb [$(\alpha,\alpha 3n)$, $(\alpha,\alpha p4n)$, $(\alpha,2\alpha n)$ and $(\alpha,2\alpha 2n)$], in order to show the applicability of the above formalism. The raw data of the experimentally measured excitation function for these reactions were taken from our earlier measurements [5].

Table 1. Growth and decay phases of the three isobars. Here the g-factors are the fractions contributing to the growth and decay of the isobars.

Term	Contributing isobar	Phases of the isobar(s)	Period of contribution	Mode of contribution
g_{13}	G	Growth of P Growth of D	$O-x$	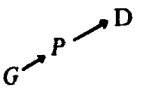
g_{12}	G	Growth of P Decay of P	$O-x$ $x-t_a$	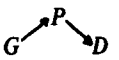
g_1	G	Decay to P Decay to D	$x-t_a$	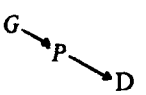
g_2	P	Growth of P Growth of D	$O-x$	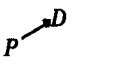
g_{23}	P	Growth of P Decay to P	$O-x$ $x-t_a$	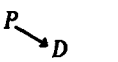
g_3	D	Growth of D	$O-x$	D

3.1 $^{93}Nb(\alpha,\alpha 3n)\,^{90}Nb$ reaction

As indicated in the inset of figure 1, there are two isobaric contributions to the residual nucleus ^{90}Nb under study. Using the present mathematical formulation, the isobaric precursor contributions, $C_g\sigma_g + C_p\sigma_p$, where C_g and C_p are the calculated coefficients and σ_g and σ_p are the experimentally measured cross-sections for the two reactions, were separated point by point. As shown in table 2, the sum of these contributions is about one third the measured cross-section around 110 MeV. The dotted curve in the figure shows the contributions which are subtracted from the experimental curve, shown by thick dashes, in order to obtain exclusively the cross-sections σ_d for the reaction under study, namely, ^{93}Nb$(\alpha,\alpha 3n)\,^{90}$Nb. Figure 9 shows a comparison between the experimentally measured cross-sections (σ_{exp}) with the exclusive cross-sections (σ_d) with the exclusive cross-sections (σ_d) obtained after separating the isobaric precursor contributions using the present mathematical formulation. Figure 9a shows that the exclusive cross-section (σ_d) is smaller by about a factor of 1·5 from the experimental cross-sections (σ_{exp}) at the peak position.

Figure 2, shows a comparison of the experimental excitation functions, so extracted, with the theoretically predicted curve on the basis of hybrid model [7,9] using the initial exciton configuration $n_0 = 4$ $(4p0h)$. As it is evident from the figure, the agreement between the theoretical predictions and the exclusive cross-sections (σ_d), shows a remarkable improvement as compared to the total experimental cross-sections (σ_{exp}), particularly in the high energy region.

3.2 $^{93}Nb(\alpha,\alpha p4n)\,^{88}Zr$ reaction

The raw experimental data along with the two important isobaric precursor contributions for this reaction are shown in figure 3. It can be seen from table 2 that, these isobaric precursor contributions are about 20% of cross-section at the maximum, that is between 90 to 100 MeV. Figure 9b shows that at the peak position, the exclusive

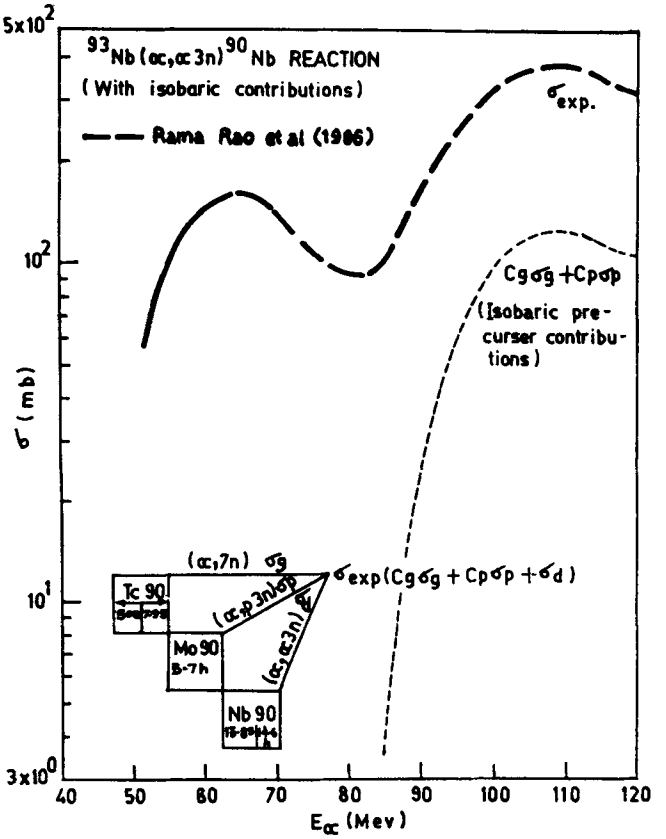

Figure 1. Experimental excitation function of ^{93}Nb(α, α3*n*) ^{90}Nb reaction. Dotted curve shows isobaric feeding of ^{93}Nb[(α, 7*n*) + (α, *p*6*n*)] reactions.

Table 2. Relative contributions of the isobaric precursors in ^{93}Nb(α, *xnypz*α) reactions. Here $C_g\sigma_g + C_p\sigma_p$ is the total isobaric precursor contributions in the experimentally measured cross-sections (σ_{exp}).

	^{93}Nb(α, α3*n*)^{90}Nb	^{93}Nb(α, α*p*4*n*)^{88}Zr	^{93}Nb(α, 2α*n*)^{88}Y	^{93}Nb(α, 2α2*n*)^{87}Y
E_α (MeV)	$\frac{C_g\sigma_g + C_p\sigma_p}{\sigma_{exp}}$	$\frac{C_g\sigma_g + C_p\sigma_p}{\sigma_{exp}}$	$\frac{C_g\sigma_g + C_p\sigma_p}{\sigma_{exp}}$	$\frac{C_g\sigma_g + C_p\sigma_p}{\sigma_{exp}}$
90	0·16	0·21	0·28	—
100	0·34	0·19	0·21	0·48
110	0·33	0·17	0·16	0·53
120	0·35	0·29	0·14	0·37

cross-sections (σ_d) is smaller by about a factor of 1·3 as compared to the experimentally measured cross-sections.

A comparison of the exclusive cross-section (σ_d) with the hybrid model predictions for this reaction is shown in figure 4. The theoretical excitation function for $n_0 = 4(4p\,0h)$ nearly reproduces the shape and also gives an agreement within a factor of 2. From the state of the art of pre-equilibrium model calculations, such a factor of two agreement is quite satisfactory for complex reactions like the present one.

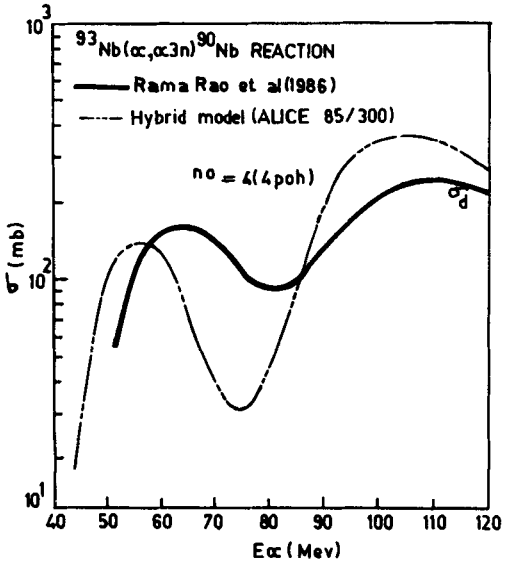

Figure 2. Comparison of theoretical results with the experimental results for $^{93}Nb(\alpha, \alpha 3n)\ ^{90}Nb$ reaction.

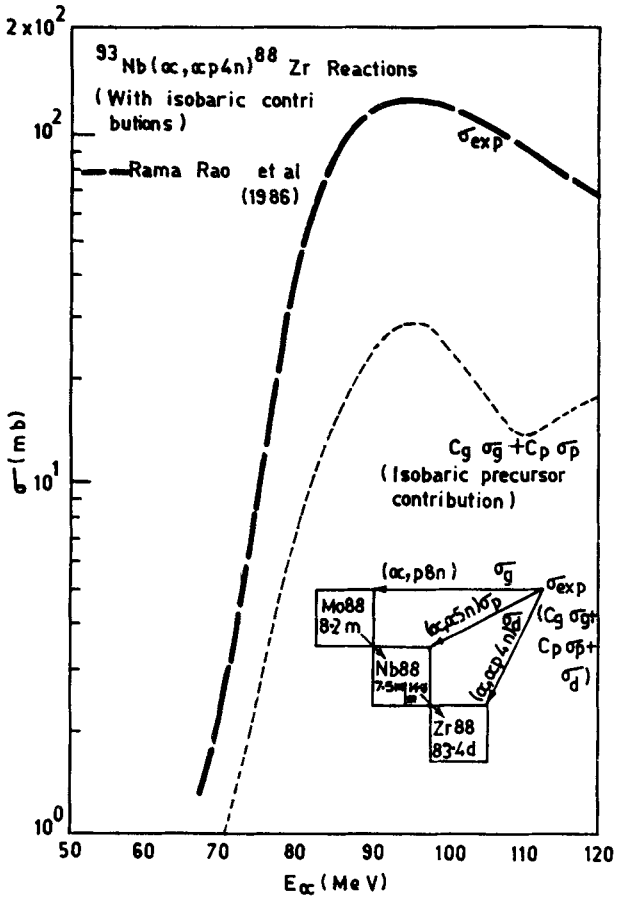

Figure 3. Experimental excitation function of $^{93}Nb(\alpha, \alpha p4n)\ ^{88}Zr$ reaction. Dotted curve shows isobaric feeding of $^{93}Nb[(\alpha, p8n) + (\alpha, \alpha 5n)]$ reactions.

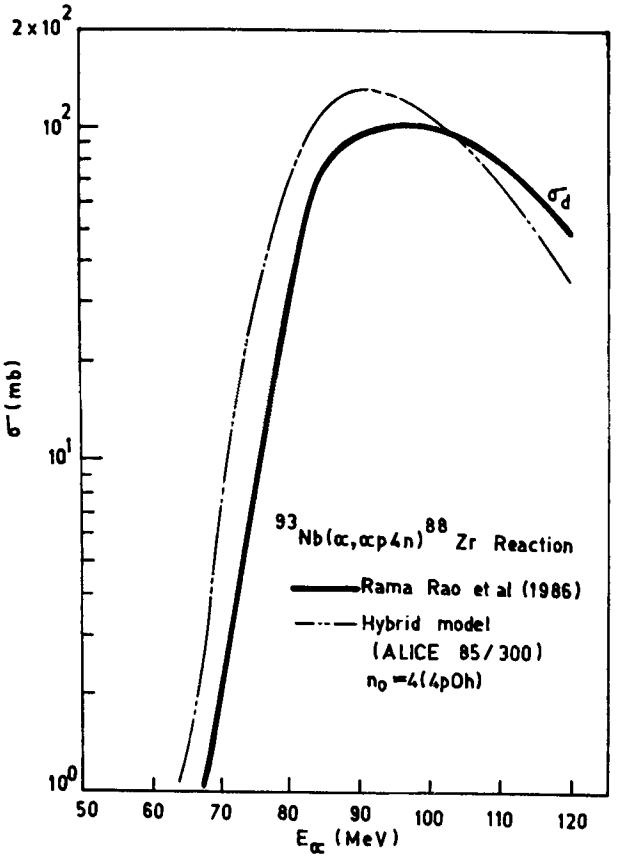

Figure 4. Comparison of theoretical results with experimental results for ^{93}Nb(α, $\alpha p4n$) ^{88}Zr reaction.

3.3 $^{93}Nb(\alpha, 2\alpha n)\ ^{88}Y$ *reaction*

The excitation function for the raw data is shown in figure 5, alongwith the isobaric precursor contributions. Table 2 shows that the isobaric precursor contribution varies between 15 and 30% in the high energy region, and exceeds the experimental errors of the measurements. Figure 9c further shows that the exclusive cross-sections (σ_d) is about a factor 1·2 smaller than the experimentally measured cross-sections (σ_{exp}).

Figure 6, shows a similar comparison between the exclusive experimental results and the hybrid model prediction for the reaction. There is a better agreement in the energy region between 80 and 120 MeV. In view of the increased alpha multiplicity, this improved agreement in the high energy region is praiseworthy.

3.4 $^{93}Nb(\alpha, 2\alpha 2n)\ ^{87}Y$ *reaction*

Figure 7, shows the excitation function for the raw data, alongwith the isobars contributing to the reaction as shown in the inset. Table 2, shows that the isobaric precursor contribution in this case is nearly 50% of the cross-section at maximum. This observation emphasizes the need for the analytical approach used in the present work. Further, it is shown in figure 9d that the exclusive cross-sections (σ_d) is almost half at the peak as compared to the experimentally measured cross-sections (σ_{exp}).

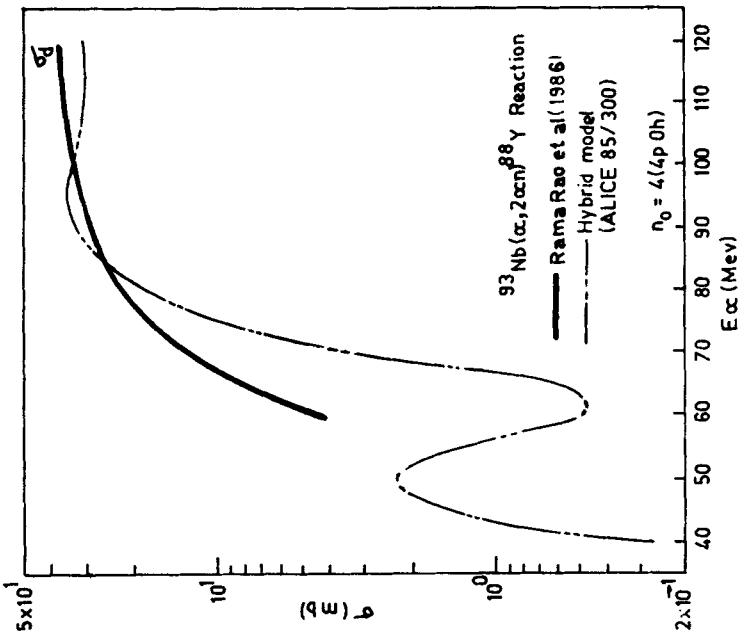

Figure 6. Comparison of theoretical results with the experimental results for ^{93}Nb(α, $2\alpha n$) ^{88}Y reaction.

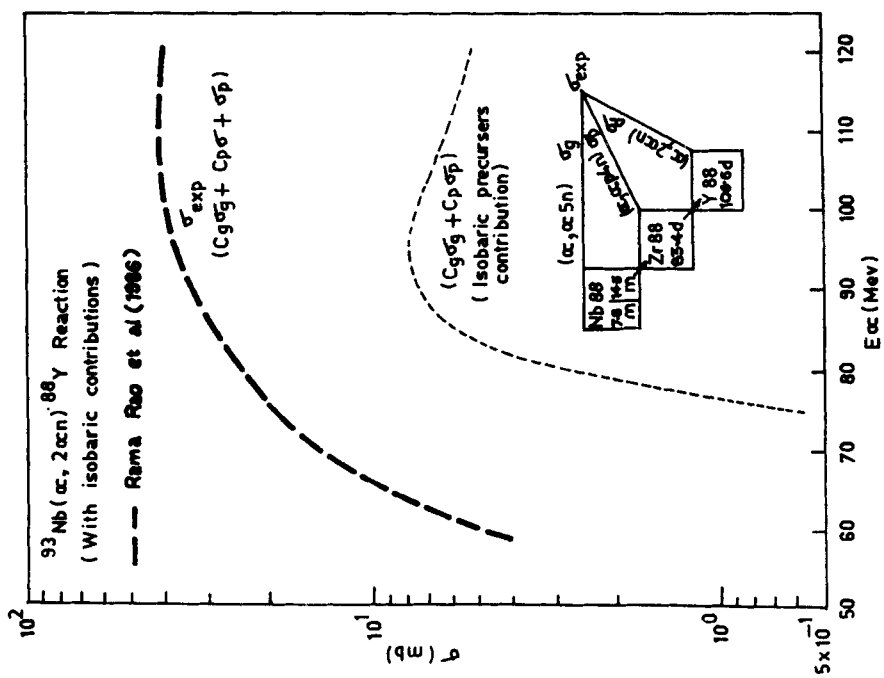

Figure 5. Experimental excitation function of ^{93}Nb(α, $2\alpha n$) ^{88}Y reaction. Dotted curve shows isobaric feeding of ^{93}Nb[(α, $\alpha 5n$) + (α, $\alpha p4n$)] reactions.

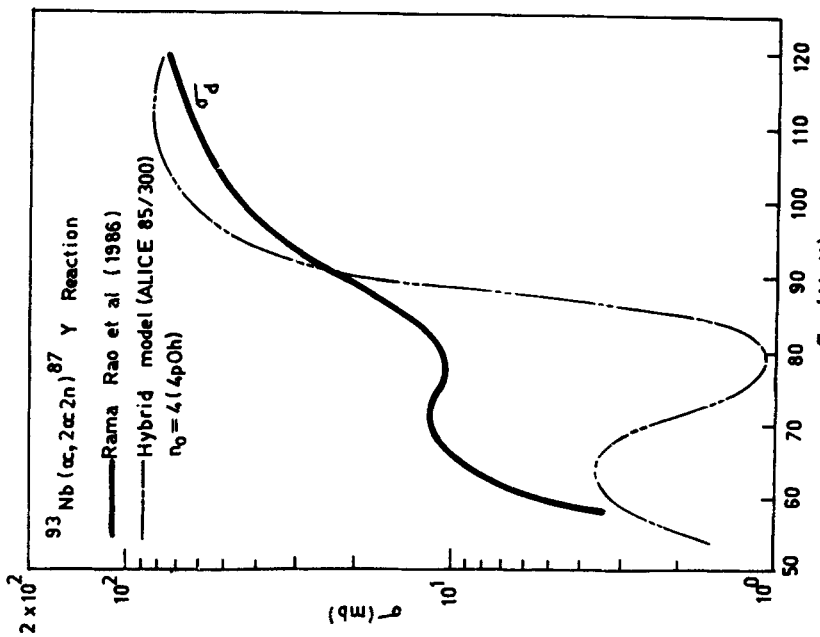

Figure 8. Comparison of theoretical results with the experimental results for ^{93}Nb(α, 2α2n) ^{87}Y reaction.

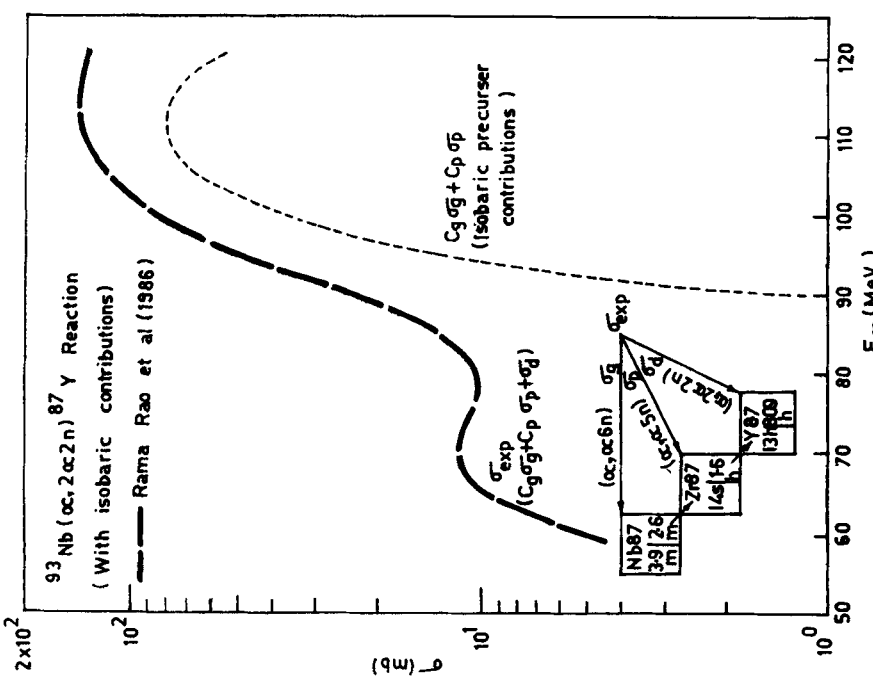

Figure 7. Experimental excitation function of ^{93}Nb(α, 2α2n) ^{87}Y reaction. Dotted curve shows isobaric feeding of ^{93}Nb[(α, α6n) + (α, αp5n)] reaction.

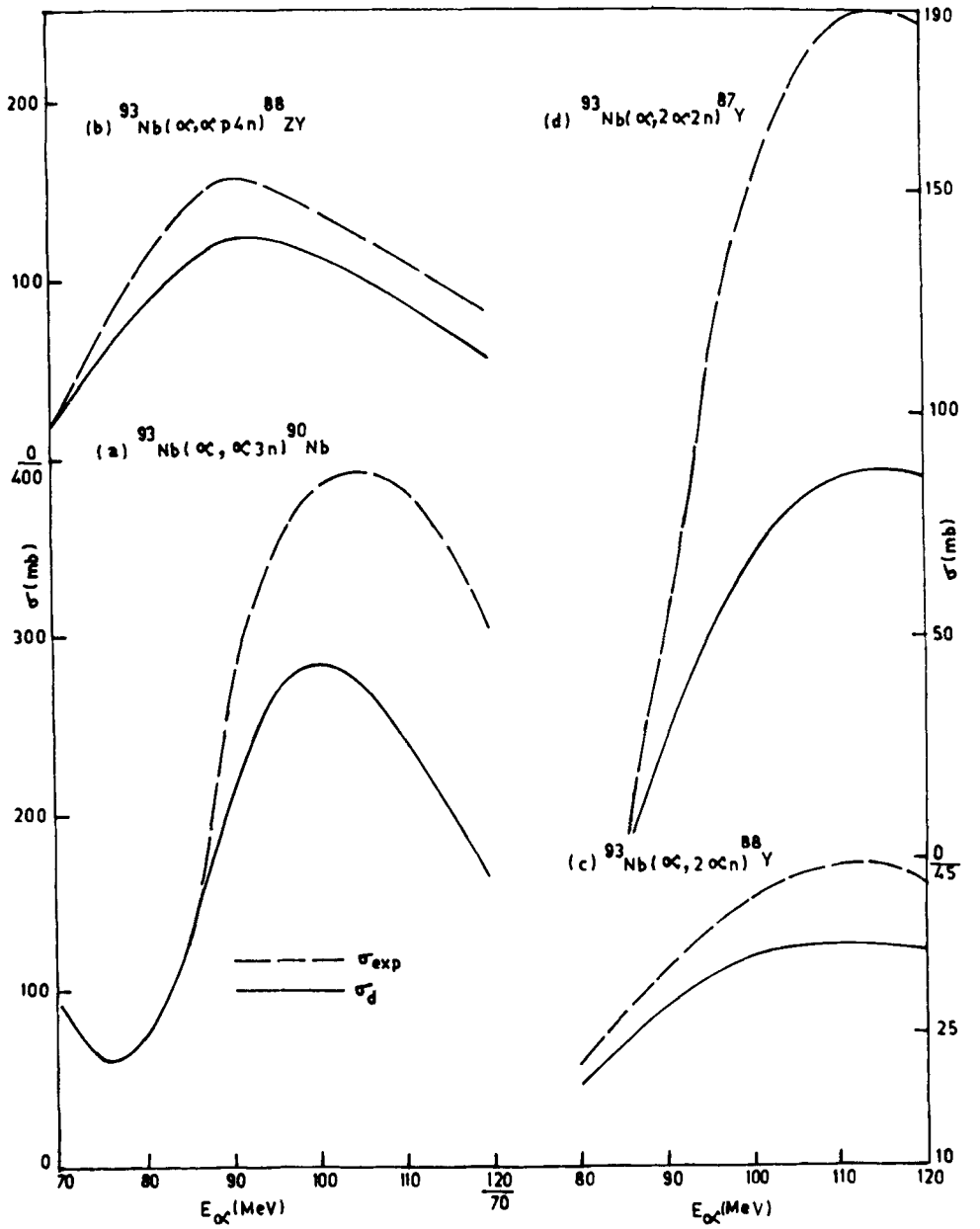

Figure 9. Comparison of the excitation functions of experimentally measured cross section (dashed curve) with the cross section excluding isobaric contributions (solid curve).

A comparison of the experimental results and the hybrid model predictions in figure 8, indicates the evidence for the emission of pre-equilibrium alpha particles around 80 MeV. At high energies beyond 90 MeV, the predicted values are reasonably close to the experimental values.

4. Conclusions

A detailed mathematical formalism is developed, to give a quantitative account of the fractional contributions of the cross-sections by the isobaric precursors, to the cross-section for the formation of the residual nucleus of interest. From the present analysis of the four reactions, namely, ^{93}Nb[$(\alpha, \alpha 3n)$, $(\alpha, \alpha p4n)$, $(\alpha, 2\alpha n)$ and $(\alpha, 2\alpha 2n)$] it can be said in general, that the present analytical formalism, separates out effectively, the isobaric precursor contributions, if any, from the (α, pxn) and $(\alpha, \alpha xn)$ type of reactions, as it is quite evident from the relatively better agreement of exclusive experimental results with the theoretical predictions of the hybrid model, particularly in the high energy (70 to 120 MeV), where the isobaric precursor contributions are prominent.

Acknowledgements

The authors are thankful to Dr V J Menon and Dr A V Mohan Rao, BHU, Varanasi, for their help and useful suggestions at various stages of this investigation. One of the authors (SM) would like to thank the MAPCOST, Bhopal, for awarding the fellowship under *FTIYS Scheme.*

References

[1] H Machner, *Phys. Lett.* **868**, 129 (1979)
[2] H Machner, *Phys. Rev.* **C21**, 2695 (1980)
[3] J Ernst, R Ibowski, H Klampl, H Machner, T Mayer Kuckuk and R Schanz, *Z. Phys.* **A142**, 545 (1982)
[4] E Gadioli, E Gadioli-Erba, J J Hogan and B V Jacak, *Phys. Rev.* **C29**, 76 (1984)
[5] J Rama Rao, L Chaturvedi, A V Mohan Rao, S Mukherjee, R Upadhyay, N L Singh, S Agarwal and P P Singh, *Proceedings of Workshop on Utilization of future programme of variable energy cyclotron*, VECC, Calcutta (India), **19**, 11 (1986)
[6] S Mukherjee, A V Mohan Rao and J Rama Rao, *Il. Nuovo Cimento* **104**, 863 (1991)
[7] M Blann and H K Vonach, *Phys. Rev.* **C28**, 1475 (1983)
[8] H Batemman, *Proc. Cambridge Philos. Soc.* **15**, 423 (1910)
[9] M Blann, Code ALICE/85/300 UCID-20169 (1984)